Purdue University
Purdue e-Pubs

International Refrigeration and Air Conditioning Conference

School of Mechanical Engineering

2014

Virtual Power Consumption and Cooling Capacity Virtual Sensors for Rooftop Units

Howard Cheung
Purdue University, United States of America, cheung@purdue.edu

James E. Braun
Purdue University, United States of America, jbraun@purdue.edu

Follow this and additional works at: http://docs.lib.purdue.edu/iracc

Cheung, Howard and Braun, James E., "Virtual Power Consumption and Cooling Capacity Virtual Sensors for Rooftop Units" (2014). *International Refrigeration and Air Conditioning Conference.* Paper 1535.
http://docs.lib.purdue.edu/iracc/1535

Virtual Power Consumption and Cooling Capacity Virtual Sensors for Rooftop Units

Howard CHEUNG*, James E. BRAUN

Ray W. Herrick Laboratories, School of Mechanical Engineering, Purdue University
West Lafayette, Indiana, U.S.A.
E-mail: cheung@purdue.edu

* Corresponding Author

ABSTRACT

Implementation of advanced controls and diagnostic features in small commercial buildings typically requires real-time monitoring of the energy flows, such as the power consumption and cooling capacity of rooftop units. However, these measurements are expensive and therefore limit the application of these advanced features. In order to lower the measurement cost, virtual sensing technology for rooftop unit power consumption and cooling capacity are being developed. Power transmitters and thermocouples are installed on the rooftop units to train the virtual sensors. The idea is to recycle the power transmitters after training to save cost, and then the virtual sensors estimate hourly electrical consumption and cooling capacity using only low cost, non-invasive temperature measurements. In this paper, development and validation of the virtual sensors are presented. The virtual power consumption sensors are validated for 2 different rooftop units installed in the field, whereas the cooling capacity sensors are validated using 4 laboratory-tested rooftop units. The reliability of the sensors is also investigated by studying the uncertainty of the virtual sensor outputs under different operating conditions. A cost comparison between the virtual sensors and direct measurement methods is also conducted to evaluate the potential for widespread application of the virtual sensing technology.

1. INTRODUCTION

Space cooling requires a lot of energy. In 2011, the U.S. spent 14.5% of its total primary energy use on space cooling in commercial buildings (Department of Energy 2011). Furthermore, about 41.3% of space cooling is provided by rooftop units (Energy Information Administration 2003). The energy consumption can be reduced by operating advanced building control and diagnostics technology. However, these technologies typically require the measurement of power consumption and cooling capacity, which are expensive and difficult to implement in the field. To reduce the cost of advanced energy-saving technologies, virtual sensors for power consumption and cooling capacity of rooftop units are developed to replace these direct measurements.

Virtual sensing technology uses measurements of other variables and mathematical models that relate the measured variables and the outputs. This approach is widely used for variables that are hard or expensive to measure directly. A detailed literature review of virtual sensors for HVAC systems was given in Li *et al.* 2011. Examples include a virtual sensor of the supply airflow of the rooftop units (Yu *et al.* 2011), a virtual sensor for water flow in pumps (Song *et al.* 2012) and a virtual sensor for refrigerant charge inside an air conditioner (Kim and Braun 2011).

In this paper, three virtual sensors are developed for retrofit to existing single-speed rooftop units to predict evaporator fan power consumption, compressor and condenser fan power consumption and cooling capacity using temperature measurements. To calibrate the sensors in the field, power transmitters and thermocouples are installed in the units to provide calibration data. After calibration, the expensive power transmitters can be reused in other units to save cost, while the thermocouples remain in the units to provide inputs for the power and cooling capacity virtual sensors. It is important to note that it is not necessary to have a direct measurement of cooling capacity in order to develop this virtual sensor. To verify the accuracy of the power consumption virtual sensors, data from 2 units in the field were used. Since it is difficult to directly measure cooling capacity in the field, the accuracy of the

cooling capacity sensor was verified with data from 4 units tested in psychrometric chambers. The calculation of the uncertainty of the virtual sensors is developed to study the reliability of the sensors, and the cost between the virtual sensing technology and direct measurement method is also compared.

2. EXPERIMENTAL SETUP

Virtual sensors were developed and evaluated for 2 rooftop units operating in the field in Philadelphia from July to September and 4 rooftop units tested in psychrometric chambers. The specification of the units in the field is tabulated in Table 1.

Table 1: Specification of systems in the field

System	1	2
Nominal cooling capacity [kW]	14.1	17.2
Refrigerant	R22	R410A
Compressor	Reciprocating	Scroll
Expansion valve	Fixed orifice	Fixed orifice

Only non-intrusive sensors were installed in the systems in Table 1. T-type Thermocouples (with an uncertainty ±0.5K) were installed on the surface of the refrigerant tubes and the condenser air inlet and outlet to measure the air temperature across the condenser, the refrigerant temperature across the heat exchangers and the condenser return bend temperature. Power transmitters (with an uncertainty ±0.1kWh per reading) were installed to measure the power consumption of the unit, and current switches were installed at the power supply of the fans and compressor to indicate which motors are operating. Data were acquired in 1-minute intervals. A schematic of the sensor installation for each unit is given in Figure 1, where T represents thermocouples, S represents current switches and W represents power transmitters.
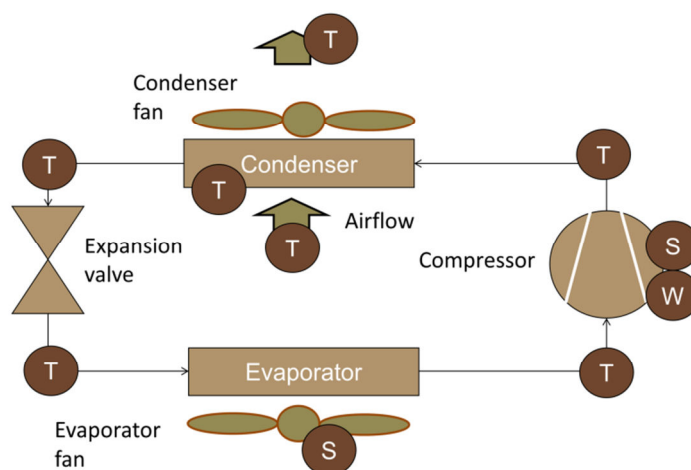

Figure 1: Schematic of sensor installation for virtual sensor calibration in the field

The laboratory data for the rooftop units came from previous studies (Breuker 1997; Shen 2006 and Kim 2013). Their specification is listed in Table 2.

Table 2: Specification of systems tested in the psychrometric chamber

System	I (Breuker 1997)	II (Shen 2006)	III (Shen 2006)	IV (Kim 2013)
Nominal cooling capacity [kW]	10.6	10.6	17.6	14.1
Refrigerant	R22	R410A	R407C	R410A

Compressor	Reciprocating	Scroll	Scroll	Reciprocating
Expansion valve	Fixed orifice	Fixed orifice	Fixed orifice	Electronic expansion valve
Valve opening control algorithm	Not applicable	Not applicable	Not applicable	Maintain an 8.7K compressor suction superheat

Unlike the units in Table 1, intrusive sensors were installed in the units in Table 2. T-type thermocouples were used to measure the refrigerant temperature along the refrigerant circuits. Grids of the thermocouples were also used to measure the air temperature across the condenser. Pressure transducers (with an uncertainty ±9.0kPa) were used to measure the pressure in the refrigerant circuit. Power transmitters (with an uncertainty ±0.5%) were installed to measure the power consumption of the fans and compressor separately. Coriolis mass flowmeters (with an uncertainty ±0.45g/s) were used to measure the refrigerant mass flow rate in the system. Other details of the experimental setup can be found in the literature (Breuker 1997; Shen 2006 and Kim 2013).

3. RELIABILITY OF THE VITUAL SENSORS

All sensors need to describe the reliability of their measurements in terms of uncertainty, and the requirement remains unchanged for virtual sensors. Song et al. (2012) and Yu et al (2011) described how the virtual sensor input uncertainty propagates to its outputs (the uncertainty from inputs), and Song et al. (2013) further described the uncertainty propagated to the sensor output from the calibration data (the uncertainty from calibration data) and the deviation between measurement and prediction (the uncertainty from deviation). In this section, two more uncertainty components, the uncertainty from outputs and the uncertainty from covariance, are introduced to quantify the repeatability of the virtual sensor prediction.

To determine the sources of the uncertainty of virtual sensor outputs, the true value of the output variable y is described as a function of a virtual sensor and an error variable ε as Eqn. (1)

$$y_{true} = f(\vec{x}, \vec{C}_{true}) + \varepsilon \tag{1}$$

Assuming that the error variable ε as Eqn. (1) follows a normal distribution with a zero mean value, the virtual sensor equation estimates the output variable by Eqn. (2).

$$y_{est} = f(\vec{x}, \vec{C}_{est}) \tag{2}$$

The regression coefficients in Eqn. (2) are usually estimated by minimizing a cost function with a set of calibration data. The process can be described as another function in Eqn. (3), where the calibration data consist of n data points.

$$\vec{C}_{est} = g(y_{cal,1}, ..., y_{cal,n}, \vec{x}_{cal,1}, ..., \vec{x}_{cal,n}) \tag{3}$$

3.1 Uncertainty from inputs
Uncertainty of the inputs to the virtual sensor propagates to its outputs. It was described in Song et al (2013) as Eqn.(4) .

$$\Delta y_{est,input} = \sqrt{\Sigma_i \left(\frac{\partial f(\vec{x}, \vec{C}_{est})}{\partial x_i} \Delta x_i \right)^2} \tag{4}$$

3.2 Uncertainty from calibration data
Song et al (2013) described how the uncertainty of the calibration data propagates to the uncertainty of the virtual sensor outputs through the calibration process in Eqn. (3), and the uncertainty propagation can be written as Eqn. (5).

$$\Delta y_{est,cal} = \sqrt{\Sigma_i \Sigma_j \left(\Sigma_k \left(\frac{\partial f(\vec{x}, \vec{C}_{est})}{\partial C_{est,k}} \frac{\partial C_{est,k}}{\partial x_{cal,i}} \right) \Delta x_{cal,i,j} \right)^2 + \Sigma_i \left(\Sigma_k \left(\frac{\partial f(\vec{x}, \vec{C}_{est})}{\partial C_{est,k}} \frac{\partial C_{est,k}}{\partial y_{cal,i}} \right) \Delta y_{cal} \right)^2} \tag{5}$$

3.3 Uncertainty from output deviation

The uncertainty from deviation of predicted and measured outputs is also described in Song et al (2013). With the definition of a 95% confidence interval, the uncertainty component is defined as Eqn. (6).

$$\Delta y_{est,dev} = t_{0.95,n-p-1}\sqrt{\frac{\Sigma_i(f(\vec{x}_{cal,i},\vec{C}_{est})-y_{cal,i})^2}{n-p-1}} \tag{6}$$

3.4 Uncertainty from covariance

While the uncertainty in Eqn. (6) estimates the uncertainty component based on the deviation between the predicted and measured output, it does not include the uncertainty due to the deviation between the true regression coefficients in Eqn. (1) and the estimated regression coefficients in Eqn. (2). Multiple books (Montgomery 2005; Graybill and Iyer 1994) described how the deviations of the coefficients are calculated by the covariance of the calibration data for linear functions. For non-linear functions such as Eqn. (1), Gallant (1975) estimated the covariance by the Jacobian of the function. The resultant equation of the uncertainty from covariance is Eqn. (7).

$$\Delta y_{est,cov} = \Delta y_{est,dev}(\frac{\partial f}{\partial \vec{C}_{est}})^T([\frac{\partial \vec{f}_{cal}}{\partial C_{est,1}} \quad \cdots \quad \frac{\partial \vec{f}_{cal}}{\partial C_{est,p}}]^T[\frac{\partial \vec{f}_{cal}}{\partial C_{est,1}} \quad \cdots \quad \frac{\partial \vec{f}_{cal}}{\partial C_{est,p}}])^{-1}(\frac{\partial f}{\partial \vec{C}_{est}}) \tag{7}$$

3.5 Uncertainty from outputs

Since Eqn. (2) is built from measured calibration data, it can only estimate the measured output variable. However, the aim of the virtual sensor is to predict the true value of its output, and the uncertainty between the virtual sensor output and the true value of the output variable should be quantified. The uncertainty from outputs is equal to the uncertainty of the sensors measuring the output variables in the calibration data. If the uncertainty of the sensors is constant, the uncertainty from outputs is provided by Eqn. (8).

$$\Delta y_{est,output} = \Delta y_{cal} \tag{8}$$

Otherwise, the uncertainty from outputs is estimated by Eqn. (9).

$$\Delta y_{est,output} = \frac{1}{n}\Sigma\frac{\Delta y_{cal,i}}{y_{cal,i}} \tag{9}$$

3.5 Overall uncertainty of the virtual sensor output

The overall uncertainty of the virtual sensor output is provided by the sum of squares of all its components as shown in Eqn. (10).

$$\Delta y_{est} = \sqrt{\Delta y_{est,input}^2 + \Delta y_{est,cal}^2 + \Delta y_{est,dev}^2 + \Delta y_{est,cov}^2 + \Delta y_{est,output}^2} \tag{10}$$

4. COOLING CAPACITY VIRTUAL SENSOR

Virtual sensors are usually calibrated by measurement data of the variables which they predict. However, cooling capacity measurement in the field is expensive, and it is infeasible to calibrate a cooling capacity sensor with measured capacity. A practical cooling capacity virtual sensor should not need measured cooling capacity for calibration. In this paper, this goal was achieved by calibrating virtual sensors of refrigerant mass flow rate and condenser airflow rate from the measurement data and predicting the cooling capacity using an energy balance on the rooftop unit.

The virtual sensor of the compressor mass flow rate is built based on the compressor mass flow rate model from Jähnig et al. (2002). By neglecting the compressor suction pressure drop, the model can be written as Eqn. (11).

$$\dot{m}_{r,comp,est,1} = \rho_{r,comp,in}(C_1 + C_2((\frac{P_{r,comp,out}}{P_{r,comp,in}})^{(1/k)}-1)) \tag{11}$$

When the measured condenser outlet subcooling is higher than its uncertainty, the compressor mass flow rate can also be estimated by an energy balance on the condenser as shown in Eqn. (12).

$$\dot{m}_{r,comp,est,2} = \frac{\rho_{a,cond,in}(T_{a,cond,in})c_{p,a,cond,in}C_5(T_{a,cond,out} - T_{a,cond,in})}{h_{r,cond,in}(T_{r,cond,in}, P_{r,cond,in}) - h_{r,cond,out}(T_{r,cond,out}, P_{r,cond,out})} \tag{12}$$

In Eqn. (12), the condenser airflow is unknown and is represented by a constant C_5, the condenser fan power is assumed to be negligible compared to the condenser heat transfer rate, the condenser air inlet density is calculated using the ideal gas law with atmospheric pressure at 101.325kPa and a constant specific capacity of air at 1.006kJ/kg-K is assumed.

The compressor mass flow rate virtual sensor in Eqn. (11) can also be used to estimate the compressor power consumption by Eqn. (13), which is the energy balance equation of the compressor.

$$\dot{W}_{comp,est,1} = \dot{m}_{r,comp,1}(h_{r,comp,out}(T_{r,comp,out}, P_{r,comp,out}) - h_{r,comp,in}(T_{r,comp,in}, P_{r,comp,in}))$$
$$+ C_3(T_{r,comp,out} - T_{a,cond,out}) + C_4(T_{r,comp,in} - T_{a,cond,out}) \tag{13}$$

The first term of Eqn. (13) on the right-handed side describes the enthalpy rise of the refrigerant flow and the remaining terms characterize the heat transfer rate between the ambient and the compressor. The equation is only applicable to conditions where the compressor suction superheat is higher than its measurement uncertainty. Otherwise, the uncertainty of the compressor suction enthalpy in Eqn. (13) and density in Eqn. (11) will be too high to estimate the compressor power consumption accurately. Since the compressors of rooftop units are usually installed at the condenser outlet, the condenser air outlet temperature is used to estimate the heat transfer rate between the compressor and the ambient.

With the measured compressor power consumption and the refrigerant property calculation package from Bell (2010), the regression coefficients in Eqns. (11), (12) and (13) can be estimated by minimizing the objective function in Eqn. (14) with the limited BFGS algorithm (Byrd 1995), where all regression coefficients are bounded to be positive to maintain their physical meaning.

$$J_1 = \Sigma_i \left(\frac{\dot{m}_{r,comp,est,1,i} - \dot{m}_{r,comp,est,2,i}}{\dot{m}_{r,comp,est,1,i}}\right)^2 + \left(\frac{\dot{W}_{comp,est,1} - \dot{W}_{comp}}{\dot{W}_{comp}}\right)^2 \tag{14}$$

After estimating the regression coefficients, the cooling capacity can be estimated by Eqn. (15).

$$\dot{Q}_{evap,est} = \rho_{a,cond,in}(T_{a,cond,in})c_{p,a,cond,in}C_5(T_{a,cond,out} - T_{a,cond,in}) - \dot{W}_{comp} - \dot{W}_{cond} \tag{15}$$

Its uncertainty calculation only involves the uncertainty from inputs and the uncertainty from calibration data as the virtual cooling capacity sensor does not involve measured cooling capacity in its calibration data and other uncertainty components cannot be defined according to Eqns. (6), (7), (8) and (9).

The output of the cooling capacity virtual sensor is compared to the measured refrigerant-side cooling capacity of systems in Table 2 and the results are plotted in Figure 2, Figure 3, Figure 4 and Figure 5.
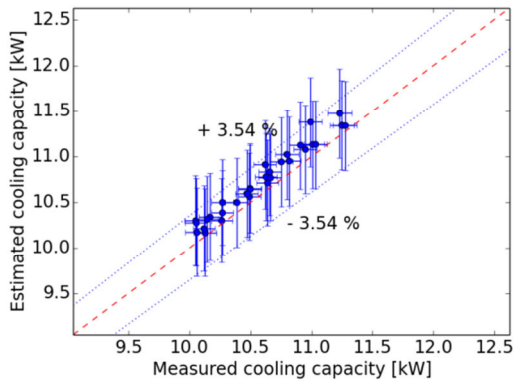
Figure 2: Comparison between the estimated and measured cooling capacity of system I
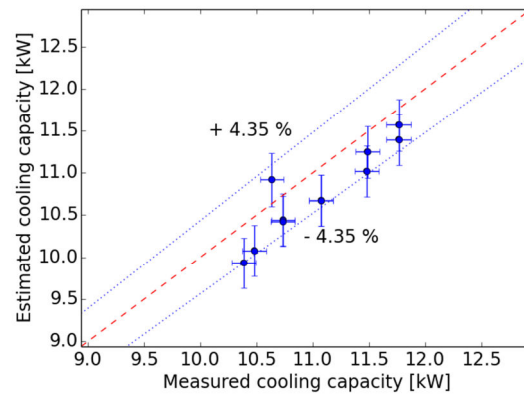

Figure 3: Comparison between the estimated and measured cooling capacity of system II
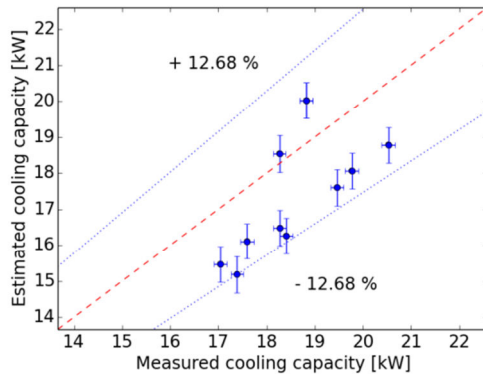

Figure 4: Comparison between the estimated and measured cooling capacity of system III
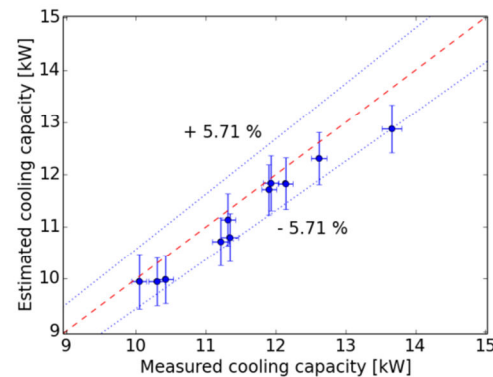

Figure 5: Comparison between the estimated and measured cooling capacity of system IV

These figures show that the estimation of cooling capacity is biased. This is unavoidable as the virtual sensor is not calibrated with measured cooling capacity and the minimization of the objective function may not eliminate the bias. However, the virtual sensor can still estimate the cooling capacity within 6% of the measured values for system I, II and IV, showing that the sensor is accurate. The 12.68% deviation in system IV is a result of inconsistent condenser airflow among its calibration data. The virtual sensor is developed assuming that the condenser airflow does not change, but the condenser airflow rates calculated from the experimental data of system III scatter around the mean value with a maximum deviation of 13.68%. The large scattering of the condenser airflow rates is too significant for Eqn. (12) to be valid and induces a large error in Figure 4.

The uncertainty of the estimation in the figures is smaller than 5% of the estimation values, showing that the estimation results are not highly sensitive to the uncertainty of the calibration data and the inputs to the sensors.

5. EVAPORATOR FAN POWER CONSUMPTION VIRTUAL SENSOR

Assuming that evaporator fans of single-speed rooftop units operate at steady state with constant power consumption, the average power consumption of the evaporator fan in the calibration data gives an unbiased estimate of the evaporator fan power consumption, and the average can be used as its virtual sensor as Eqn. (16).

$$\dot{W}_{evap,est} = \frac{1}{n} \Sigma_i \dot{W}_{evap,i} \tag{16}$$

Evaporator fans of rooftop units often operate when the compressor and condenser fan are off. Measuring the power consumption of the rooftop units during this time provides data to calibrate evaporator fan power consumption virtual sensors without the need for additional power transmitters. To test the accuracy and reliability of the evaporator fan power consumption virtual sensor, they were calibrated using data from the units listed in Table 1 for 23 days in August 2013 and the estimation results of the virtual sensors were tabulated in Table 3.

Table 3: Estimation results of evaporator fan power consumption virtual sensor

System	Estimated power [kW]	Relative uncertainty of the power transmitter	Relative uncertainty of the virtual sensor	Coefficient of variation	Number of data points
1	0.78	2.31%	4.34%	1.83%	58
2	0.95	1.76%	3.85%	1.71%	63

The coefficient of variation in Table 3 is a ratio of the mean square error of the virtual sensor to its mean estimated power consumption, and their small magnitudes (less than 2%) show that the virtual sensors are accurate. Although the uncertainty of the virtual sensor output is higher than that of the uncertainty of the power transmitter, the uncertainty of the virtual sensors is smaller than 5%.

6. COMPRESSOR AND CONDENSER FAN POWER CONSUMPTION VIRTUAL SENSOR

Similar to the evaporator fans, the condenser fans of single-speed rooftop units do not change power consumption significantly with environmental conditions. However, they operate together with the compressor and the setup in Figure 1 cannot measure the condenser fan power consumption separately from the compressor power consumption. To accommodate the situation, a virtual sensor is built to estimate the combined power consumption of the condenser fan and compressor.

To build the virtual sensor, a compressor power consumption model is needed. Since the compressor suction superheat is not always smaller than its measurement uncertainty during compressor operation, the virtual sensor cannot use the model in Eqn. (13), and another model is needed. By including the effect of compressor discharge pressure within the compressor isentropic efficiency model of Jähnig et al. (2002), the isentropic efficiency can be estimated by Eqn. (17).

$$\eta = C_6 + C_7 exp(C_8 P_{r,comp,in}) + C_9 exp(C_{10} P_{r,comp,out}) \tag{17}$$

Since the condenser fan does not need to overcome flow resistance in air ducts, its fan power is smaller than the evaporator fan power consumption and small compared to the compressor power consumption. Thus, the combined power consumption can be adequately estimated using the compressor power consumption model form from Jähnig et al. (2002) as shown in Eqn. (18).

$$\dot{W}_{comp,est,2} + \dot{W}_{cond,est} = \frac{1}{\eta}(C_1 + C_2((\frac{P_{r,comp,out}}{P_{r,comp,in}})^{(1/k)} - 1)\frac{k}{k-1}P_{r,comp,in}((\frac{P_{r,comp,out}}{P_{r,comp,in}})^{(1-\frac{1}{k})} - 1) \tag{18}$$

The regression coefficients in Eqn. (17) can be estimated by minimizing the objective function Eqn. (19), where C_1 and C_2 are estimated during the calibration of the cooling capacity virtual sensor.

$$J_2 = \Sigma_i(\frac{(C_1 + C_2((\frac{P_{r,comp,out,i}}{P_{r,comp,in,i}})^{(1/k_i)} - 1)\frac{k_i}{k_i-1}P_{r,comp,in,i}((\frac{P_{r,comp,out,i}}{P_{r,comp,in,i}})^{(1-\frac{1}{k_i})} - 1)}{\dot{W}_{comp,i} + \dot{W}_{cond,i}} - \eta_i)^2 \tag{19}$$

To calibrate the virtual sensor for units where refrigerant pressure is not measured, such as the units in Table 1, virtual pressure sensors (Li et al. 2011) are used to estimate the compressor suction pressure by the saturation pressure at the evaporator inlet temperature and the compressor discharge pressure by the saturation pressure at the condenser return bend temperature.

The accuracy and reliability of the virtual compressor and condenser fan power sensors were tested based on 30-minute steady state data for the units in Table 1, and the results are plotted in Figure 6 and Figure 7.
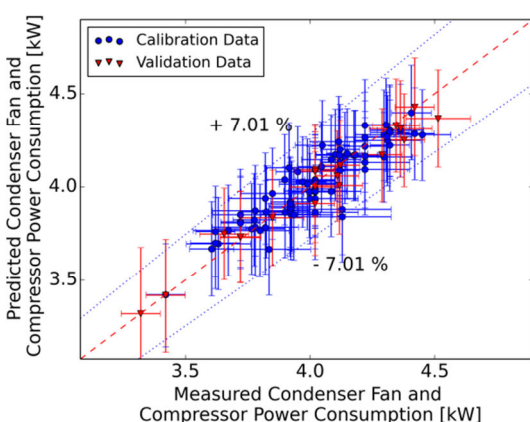

Figure 6: Comparison between the estimated and measured power consumption of the compressor and condenser fan of system 1
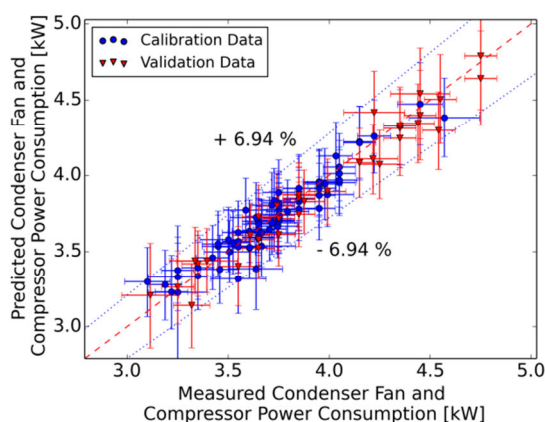
Figure 7: Comparison between the estimated and measured power consumption of the compressor and condenser fan of system 2

The results in Figure 6 and Figure 7 cover two different periods. The calibration data were acquired in August 2013 for 23 days to calibrate the virtual sensors, and validation data were acquired in September 2013 for 7 days and were not used for virtual sensor calibration. Both figures show that the combined power consumption can be estimated within about 7% of the measured values for both the calibration and validation period. The coefficients of variation of virtual sensors of system 1 and 2 are 2.40% and 2.41% respectively. This shows that the virtual sensors are accurate. The relative uncertainty of the virtual sensors of system 1 and 2 are 6.12% and 5.95%, respectively.

With virtual sensors for fan and compressor power consumption, hourly energy consumption for the rooftop units were estimated by integrating the virtual sensor reading every minute, including the readings during unsteady operation. The results are plotted in Figure 8 and Figure 9.
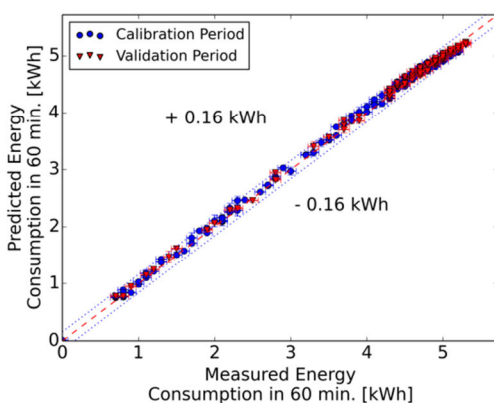

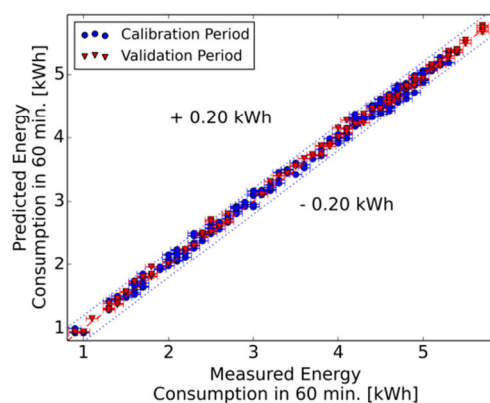**Figure 8:** Comparison between the estimated and measured hourly energy consumption of system 1

Figure 9: Comparison between the estimated and measured hourly energy consumption of system 2

The estimation deviates from the measured value by 0.16kWh in Figure 8 and 0.20kWh in Figure 9, showing that the integration of virtual sensor readings can estimate the hourly energy consumption of the rooftop units in unsteady operation accurately. Due to integration, the average uncertainty of the estimated hourly energy consumption is 0.02kWh.

7. COST COMPARISON BETWEEN MEASUREMENT AND VIRTUAL SENSING

To evaluate the potential for virtual sensing technology to decrease implementation costs, estimates of the costs for direct measurement and virtual sensing of power consumption and cooling capacity were compared. The scenarios for the cost comparisons are described in Table 4 and Table 5. It is assumed that 3x3 grids of thermocouples are needed to provide reasonable accuracy for air inlet and outlet temperatures.

Table 4: Scenarios of measurement and virtual sensing technology

Direct measurement	Virtual sensing technology
1 power transmitter for each unit to measure the total power consumption	1 power transmitter for each unit during the calibration process only
18 thermocouples (3x3 grids) to measure the air temperature difference across the evaporator per unit	18 thermocouples (3x3 grids) to measure the air temperature difference across the condenser and 5 thermocouples for refrigerant temperatures per unit
2 relative humidity sensors for humidity across the evaporator per unit	2 current switches to show the operating status of evaporator and compressor per unit
1 airflow measurement stations with multiple hot-wire anemometers for evaporator airflow per unit	18 hours of technician work per unit
4 hour of technician work per unit	

Table 5: Assumptions of cost for items in the business scenarios

Power transmitter	$500/ sensor	Hot-wire anemometers	$1600/ station
T-type thermocouples	$50/ sensor	Current switch	$50/ sensor
Relative humidity sensor	$240/ sensor	Technician salary	$70/ hour

It is assumed that the power transmitters used for calibrating the virtual sensors would be shared by multiple units to save cost. Assuming a calibration period for 23 days for each sensor, each power transmitter could be shared by 15 units per year. Technicians need to spend more time installing the virtual sensors than the direct measurement because the installation of the thermocouples on the refrigerant circuit is difficult due to the geometry and location of the heat exchangers in the unit. In addition, the technician must return to the site and remove the power transmitter after calibration. The cost savings for the virtual sensor relative to direct measurement depends on the time required for a technician to set up the virtual sensors in the field. If it takes 20 hours of technician time per unit, then the cost savings would be $1100 per unit for the scenarios of Table 4 and Table 5. The break-even point (zero savings) occurs for a technician time of 35 hours per unit.

8. CONCLUSIONS

To conclude, accurate power consumption and cooling capacity virtual sensors were developed that could be applied as retrofits to existing rooftop units in field. The virtual sensors can be calibrated using field measurements of power consumption and temperature only. After calibration, the power transmitters can be removed from the units to save cost. Then, the virtual sensors rely on temperature and on/off status to estimate the power consumption and cooling capacity. To evaluate the reliability of the virtual sensor outputs, uncertainties were calculated that include the effects of the uncertainties in the inputs, calibration data, output prediction and measurement deviation, covariance and output measurement. The virtual sensors were created based on an energy balance and compressor models, and their accuracy and prediction reliability were examined using data collected from 2 units operating in the field and 4 units tested in psychrometric chambers. Although there was a small bias in the cooling capacity estimation, the virtual sensors could estimate hourly energy consumption and cooling capacity of the rooftop units accurately and reliably. The cost of the virtual sensing technology was also compared to direct measurement and the cost savings appear to be significant for application to retrofits.

NOMENCLATURE

C	regression coefficients	(varies)	n	number of calibration data points	(--)
c_p	specific heat capacity	(kJ/kJ-K)	P	pressure	(kPa)
ε	error variable	(varies)	Q	heat transfer rate	(kW)
η	isentropic efficiency	(--)	ρ	density	(kg/m^3)

f	function for virtual sensors	(varies)	T	temperature	(K)
g	function for regression coefficient estimation	(varies)	t	t-statistics	(--)
h	enthalpy	(kJ/kg)	W	power consumption	(kW)
J	objective function	(--)	x	input variable	(varies)
k	specific heat ratio at compressor suction	(--)	y	output variable	(varies)
m	mass flow rate	(kg/s)			

Subscript

a	air	in	inlet
cal	calibration	input	input
comp	compressor	out	outlet
cond	condenser	output	output
dev	deviation	r	refrigerant
est	estimation	true	true
evap	evaporator		

REFERENCES

Bell, I. H., 2011, Coolprop: Fluid properties for the masses, retrieved from http://coolprop.sourceforge.net/

Breuker, M., 1997, Evaluation of a Statistical, Rule-based, Detection and Diagnostics Method for Vapor Compression Air Conditioners, Master thesis, Ray W. Herrick Laboratories, Purdue University, Ind. Report No. 1796-6

Byrd, R. H., Lu, P., Nocedal, J., 1995, A Limited Memory Algorithm for Bound Constrained Optimization, *SIAM Journal on Scientific and Statistical Computing*, 16: p. 1190 - 1208

Department of Energy, 2011, 2011 Buildings Data Book

Energy Information Administration, 2003, 2003 Commercial Building Energy Consumption and Expenditures

Gallant, 1975, Nonlinear Regression, *The Am. Stat.*, 29: p.73 - 81

Graybill, F. A., Iyer, H. K., 1994, *Regression Analysis: Concepts and Applications*, 1st Edition, Duxbury Pr

Jähnig, D. I., Reindl, D. T., Klein, S. A., 2000, A semi-empirical method for representing domestic refrigerator/freezer compressor calorimeter test data, *ASHRAE Trans.*, 106: p. 112 - 130

Kim, W., Braun, J. E., 2012, Performance evaluation of a virtual refrigerant charge sensor, *Int. J. of Refrig.*, 36: p.1130-1141

Kim, W. 2013, *Fault Detection and Diagnosis for Air Conditioners and Heat Pumps based on Virtual Sensors*, PhD thesis, Ray W. Herrick Laboratories, Purdue University

Li, H., Yu, D., Braun, J. E., A review of virtual sensing technology and application in building systems, *HVAC&R Res.*, 17: p. 619 - 645

Montgomery, D. C., 2005, *Design and Analysis of Experiments*, 6th Edition, Jon Wiley & Sons

Shen, B., 2006, Improvement and validation of unitary air conditioner and heat pump simulation models at off-design conditions, Ph.D. thesis, Ray W. Herrick Laboratories, Purdue University, Ind. Report No. 6304-1 HL2006-1

Song, L., Joo, I., Wang, G., 2012, Uncertainty analysis of a virtual water flow measurement in building energy consumption monitoring, *HVAC&R Res.*, 18: p. 997 - 1010

Song, L., Wang, G., Brambley, R., 2013, Uncertainty analysis for a virtual flow meter using an air-handling unit chilled water valve, *HVAC&R Res.*, 19: p. 335-345

Yu, D., Li, H., Yang, M., 2011, A virtual supply airflow rate meter for rooftop air-conditioning units, *Build. and Enviorn.*, 46: p. 1292-1302

ACKNOWLEDGEMENT